ISSN (Print) 1226-1750
ISSN (Online) 2233-6656
Journal of Magnetics 23(1), 68-73 (2018) https://doi.org/10.4283/JMAG.2018.23.1.068

Experimental Assessment of Unbalanced Magnetic Force according to Rotor Eccentricity in Permanent Magnet Machine

Jeong-Jin Yoo[1], Seung-Han Lee[1], Kyung-Hun Shin[2], and Han-Wook Cho[1]*

[1]Department of Electric, Electronic and Communication Eng. Edu., Chungnam National University, Daejeon 34134, Republic of Korea
[2]Department of Electrical Engineering, Chungnam National University, Daejeon 34134, Republic of Korea

(Received 21 February 2017, Received in final form 22 January 2018, Accepted 23 January 2018)

The manufacturing errors of machine tools are usually due to the imperfect of bearings, stiffness of spindle, assembly errors, and so on. In addition, the rotor eccentricity of the permanent magnet (PM) machine affects to the constant torque and speed characteristic of mechanical loads. The errors due to rotor eccentricity is caused by manufacturing process and rotor eccentricity generate unbalanced magnetic force (UMF). The sources of UMF are generated by the interaction between the rotor magnets and the stator core. Firstly, we suggested that the characteristic analysis results due to rotor eccentricity are calculated by using finite-element (FE) analysis. Moreover, we proposed experimental set to measure the UMF on the PM machines. Finally, we verified the validity of the proposed UMF measurement system by comparison with the measured results and simulation results due to the rotor eccentricity in the PM machine.

Keywords : permanent magnet machine, rotor eccentricity, unbalanced magnetic force

1. Introduction

Permanent magnet (PM) machines are becoming popular in various applications due to their high performance and higher operating efficiency in comparison to conventional electrical machines such as dc and induction motors [1]. In particular, rotor precision is one of the most essential components in a PM machine because the rotor is important for the operation performance, efficiency, and reliability of the motor drive system. Inevitably, however, rotor errors due to imprecision in the manufacturing process are introduced mechanically in the PM machines [2]. These types of errors generate rotor eccentricity, which causes the unbalancing of the air-gap length between the rotor magnets and stator core on the PM machine. The errors due to rotor eccentricity can cause deterioration to the performance of the PM machine. Additionally, the prediction and measurement of the unbalanced force are essential in order to maintain the high performance and efficiency of the PM machines. Therefore, investigating rotor eccentricity is important because its prediction can be made by considering the mechanical loss of wear on the bearing, as well as acoustic noise and vibration [3]. In previous studies, the rotor eccentricity with regard to vibration and acoustic noise was difficult to measure for the purpose of improving the rotation precision in the PM machines. Various researchers have indirectly predicted the existence and characteristics of the unbalanced force through the measured vibration or acoustic noise in the PM machine.

In order to confirm the experimental results of the magnitude of the unbalanced magnetic force according to the eccentricity of the rotor, it was necessary to have a model of the large air gap and the magnetic unbalance. The PM machine model of the large magnetic unbalance was selected by comparison to magnetic unbalance models reported in the literature. Hence, the 4-pole and 15-slot model with a sufficiently large magnetic unbalance was selected. Then, the characteristic variations due to rotor eccentricity were calculated for the PM machine with 4-poles and 15-slots by using finite-element (FE) analysis.

We propose an experimental setup for measuring the UMF characteristics in the PM machine. By using the proposed setup, the validity of the UMF measurement system was verified by comparing the experimental results to the simulation results of rotor eccentricity.

*Corresponding author: Tel: +82-42-821-8581
Fax: +82-42-821-8886, e-mail: hwcho@cnu.ac.kr

2. Unbalanced Magnetic Force in PM Machine

Figure 1 shows a schematic representation of rotor eccentricity. Accordingly, the eccentricity of the rotor, centers of the rotor magnet, and stator core, were different, and the air gap condition of the PM machine was unbalanced [5]. Since the rotating center was fixed by the rotating shaft, the rotor center was changed due to rotor eccentricity. If the center of the rotor was moved as much as the rotor eccentricity, the obtained results indicated that the PM machine characteristics were affected by the variation of the air-gap length, which was caused by rotor eccentricity [6]. Rotor eccentricity also affected various other characteristics of the PM machine, such as the electromagnetic force characteristics. The total magnetic force on the body placed within the electromagnetic field could be calculated by integrating the magnetic stress on the closed surface around the body. The electro-magnetic forces on the object surface in the magnetic field are expressed by [7]:

$$\vec{F} = \frac{1}{\mu_0}(\vec{B}_n^{\,2} - \frac{1}{2}|\vec{B}|^2)\vec{i}_n + \frac{1}{\mu_0}\vec{B}_n\vec{B}_t\,\vec{i}_t \quad (1)$$

where B is the magnetic flux density, and n and t represent the normal and tangential components in the coordinate system, respectively.

Owing to the assumption of an infinitely permeable stator and rotor iron in the PM machine, the radial and tangential magnetic local traction acting on the stator surface could be obtained based on the Maxwell stress tensor, as follows:

$$\vec{f}_n = \frac{1}{2\mu_0}(\vec{B}_{rg}^{\,2} - \vec{B}_{\theta g}^{\,2}) \quad (2)$$

$$\vec{f}_t = \frac{1}{2\mu_0}\vec{B}_{rg}^{\,2}\vec{B}_{\theta g} \quad (3)$$

where in the polar coordinate system, B_{rg} and $B_{\theta g}$ represent the radial and tangential components of the magnetic flux density, respectively, which can be converted to a system of Cartesian coordinates, as follows:

$$\vec{f}_x = \vec{f}_r \cos\theta - \vec{f}_r \sin\theta \quad (4)$$

$$\vec{f}_y = \vec{f}_r \sin\theta - \vec{f}_\theta \cos\theta \quad (5)$$

Due to the influence of rotor eccentricity, the components of the unbalanced magnetic force acting on the stator center of the PM machine were calculated over the circular surface of the radius in the middle of the air gap region.

The unbalanced magnetic force in the x-axis and y-axis directions, respectively, is expressed as follows:

$$\vec{F}_x = \frac{rl_{stk}}{2\mu_0}\int_0^{2\pi}\left[(\vec{B}_{\theta g}^{\,2} - \vec{B}_{rg}^{\,2})\cos\theta + 2\vec{B}_{rg}^{\,2}\vec{B}_{\theta g}^{\,2}\sin\theta\right]d\theta \quad (6)$$

$$\vec{F}_y = \frac{rl_{stk}}{2\mu_0}\int_0^{2\pi}\left[(\vec{B}_{\theta g}^{\,2} - \vec{B}_{rg}^{\,2})\sin\theta + 2\vec{B}_{rg}^{\,2}\vec{B}_{\theta g}^{\,2}\cos\theta\right]d\theta \quad (7)$$

3. FE Analysis of Rotor Eccentricity

3.1. Analysis model

The FE analysis model of the surface-mounted PM machine with 4-poles and 15-slots was designed in order to analyze the unbalanced force according to rotor eccentricity. The two models of the considered PM machine are shown in Fig. 2, where the normal condition is illustrated in Fig. 2(a), while the rotor eccentricity condition (x-axis: 1.5 mm, y-axis: 1.5 mm) of the PM machine is illustrated in Fig. 2(b). The unbalanced air-gap length affects the characteristics due to the rotor eccentricity of the PM machine. The characteristic variations due to rotor eccentricity were calculated by using FE analysis. Hence, we present the simulation results of the charac-

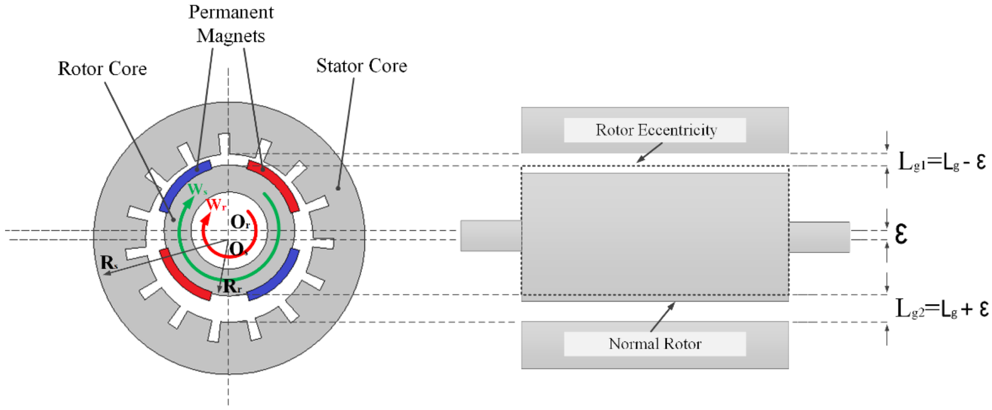

Fig. 1. (Color online) Schematic representation of rotor eccentricity in PM machine.

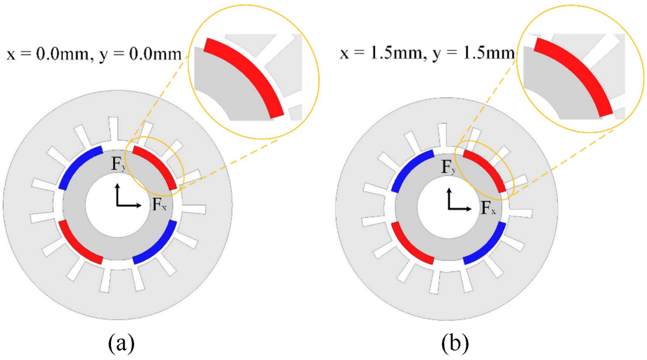

Fig. 2. (Color online) Analysis model with or without rotor eccentricity: (a) normal condition; (b) rotor eccentricity condition.

teristics variation due to the rotor eccentricity in the PM machine. The FE analysis model considered a rotor eccentricity of 0 to 150 μm. Table 1 presents the major design specifications of the analysis model.

3.2. Back-EMF and flux density

The simulation results of the back-EMF and THD due to the rotor eccentricity of 0 to 150 μm are shown in Fig. 3. The simulation results of the back-EMF analyzed the characteristics at the low speed of 60 rpm, and confirmed that the simulation results due to the rotor eccentricity were in good agreement. Table 2 lists the resultant characteristic values of back-EMF and THD due to the rotor eccentricity of 0 to 150 μm. Through the simulation results of the back-EMF, the measurement and prediction

Table 2. Simulation results of back-EMF and THD characteristics due to rotor eccentricity.

Item	Rotor eccentricity			
	0 μm	50 μm	100 μm	150 μm
Back-EMF$_{max}$ (mv)	975.24	975.06	975.19	975.22
THD (%)	5.496	5.499	5.50	5.499

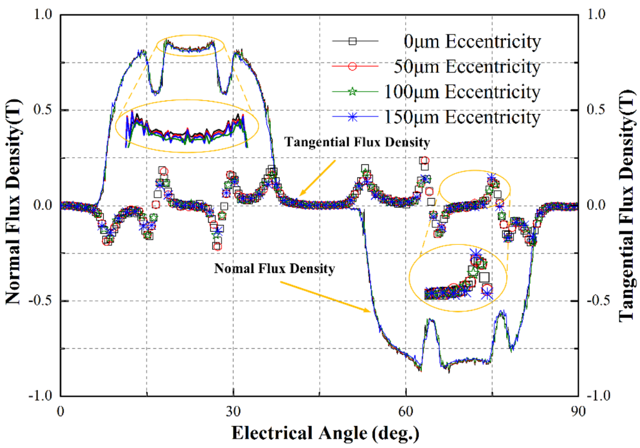

Fig. 4. (Color online) Simulation results of flux density due to rotor eccentricity.

Table 1. Specifications of analysis model.

Item	Value	Item	Value
Number of slots/poles	4/15	Thickness of PM	6 mm
Inner radius of PM	41.5 mm	Outer radius of PM	47.5 mm
Outer radius of stator	42.5 mm	Outer radius of rotor	88.35 mm
Axial length	12.7 mm	Shaft radius	25 mm
Air gap length	2.5 mm	PM remanence	1.21 T

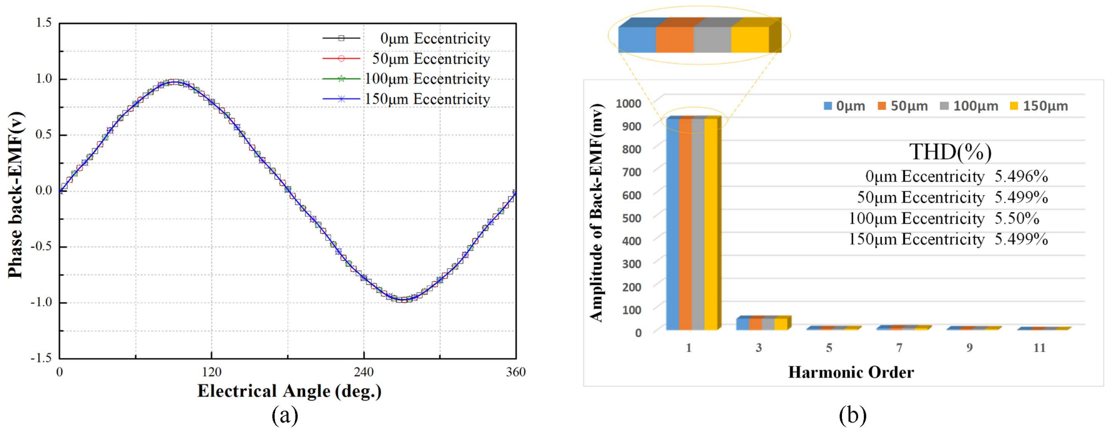

Fig. 3. (Color online) Simulation results due to rotor eccentricity of 0 to 150 μm: (a) back-EMF; (b) THD of back-EMF.

of rotor eccentricity confirmed the difficulty of detecting manufacturing errors by the rotor eccentricity of the PM machine. Figure 4 shows the flux density with rotor eccentricity between the rotor magnet and stator core in the PM machine. Additionally, the simulation results of flux density were compared according to the rotor eccentricity of 0 to 150 μm. Through the flux density of simulation results, it was practically difficult to measure the manufacturing errors due to rotor eccentricity by means of flux density measurement. As can be seen from the simulation results of the back-EMF and flux density, the simulation results due to rotor eccentricity did not influence the variation of characteristics. As a result, we confirmed that the detection of rotor eccentricity was difficult to be carried out by using the back-EMF measurement and flux density characteristics.

3.3. Cogging torque and electromagnetic torque

The torque characteristic is an important element in the manufacturing and performance testing of the PM machine. Therefore, the reduction of the cogging torque and torque ripple was investigated in order to improve the performance of electric machines [6]. Figure 5(a)-(b) shows the cogging torque and electromagnetic torque characteristics due to the rotor eccentricity of 0 to 150 μm. The results indicated that the rotor eccentricity affected the analysis results of the PM machine. Table 3 lists the simulation results of torque characteristics due to the rotor eccentricity of 0 to 150 μm. In the case of cogging torque, the simulation results due to rotor eccentricity indicated a difference of almost 5.5 mN·m, in comparison to the simulation results of 0 and 150 μm. Moreover, a resultant value greater than 0 μm and 150 μm was obtained by comparing the torque ripple characteristics due to rotor eccentricity. Consequently, as the rotor eccentricity increased, the simulation results of the torque also increased gradually.

Table 3. Simulation results of torque characteristic due to rotor eccentricity.

Item	Rotor eccentricity			
	0 μm	50 μm	100 μm	150 μm
Max torque (N·m)	1.563	1.564	1.566	1.568
Avg. torque (N·m)	1.550	1.549	1.549	1.549
Torque ripple (N·m)	0.032	0.036	0.038	0.041
Ripple ratio (%)	20.4	22.7	24.2	26.3
Cogging torque (mN·m)	9.38	10.37	11.73	14.88

Therefore, it was possible for the measurement system to predict and detect the rotor eccentricity by using the electromagnetic torque characteristic. However, when measuring the rotation accuracy due to rotor eccentricity in the PM machine by using the electromagnetic torque characteristics, the measurement system of the rotation accuracy had difficulty in constructing the experimental setup and measuring the existence of error due to rotor eccentricity [8]. Additionally, the measurement system had a very complex structure and was very expensive since it required the experimental set-up to be built as ultra-precision measuring equipment.

4. Force Measurement System

The errors due to rotor eccentricity can cause unbalance to the PM machine force. Therefore, we propose an experimental setup for measuring the UMF characteristics due to rotor eccentricity [9]. This setup was verified in practice by conducting an actual experiment.

Figure 6(a)-(b) shows the UMF measurement system diagram and implementation environment. The analysis model was operated under a no load condition by using a speed control motor (K9P180B GGM Ltd.) at low speed. We developed a measurement system that was used to

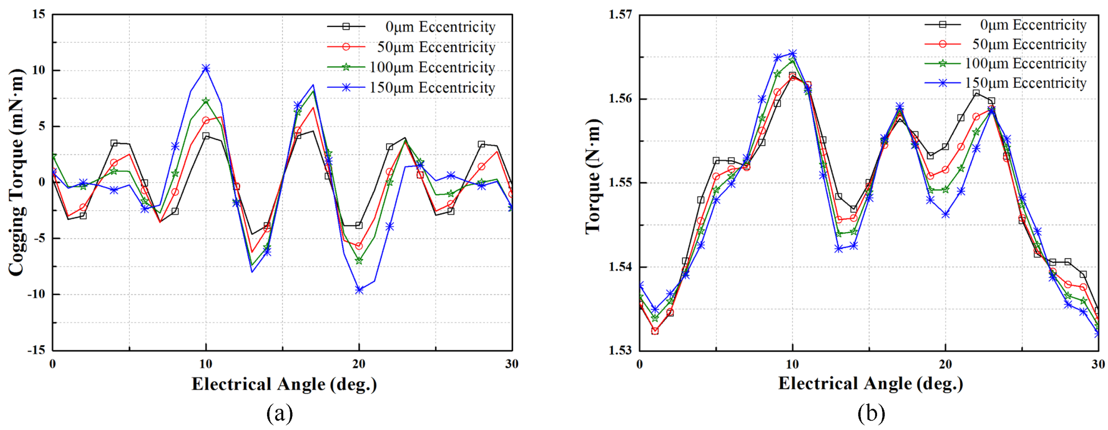

Fig. 5. (Color online) Torque characteristic analysis due to rotor eccentricity of 0 to 150 μm: (a) cogging torque; (b) torque.

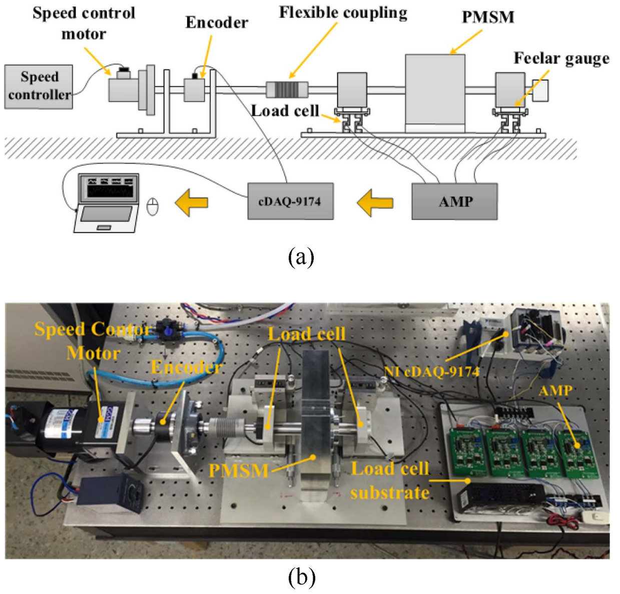

Fig. 6. (Color online) UMF experimental set-up: (a) diagram; (b) implementation environment.

measure the UMF after the rotor was separated from a stator of the PM machine. The rotor of the PM machine was connected to the rotating shaft in order to regulate the rotor eccentricity by using the feeler gauge in the Y-axis direction. The UMF measurement was performed by connecting the load cell (UU2-K50 DACELL Ltd.) to the bottom of the rotor. The load cell was connected to the amplifier with an NI cDAQ-9174 chassis. The position and speed of the rotor were measured in sequence by using a high-resolution incremental encoder. Furthermore, we monitored the UMF measurement results in real-time by using LabVIEW S/W. Therefore, the UMF measurement according to rotor eccentricity was implemented by LabVIEW S/W installed on a PC, and we performed an experiment to measure the UMF due to rotor eccentricity by using the proposed experimental setup.

5. Results and Discussion

We established that the characteristics vary according to rotor eccentricity by using the commercial FE analysis software called S/W Ansys EM. Toolkit. Additionally, we presented the simulation results, such as the force, back-EMF, flux density, and torque, on the PM machine. To measure the unbalanced force due to rotor eccentricity,

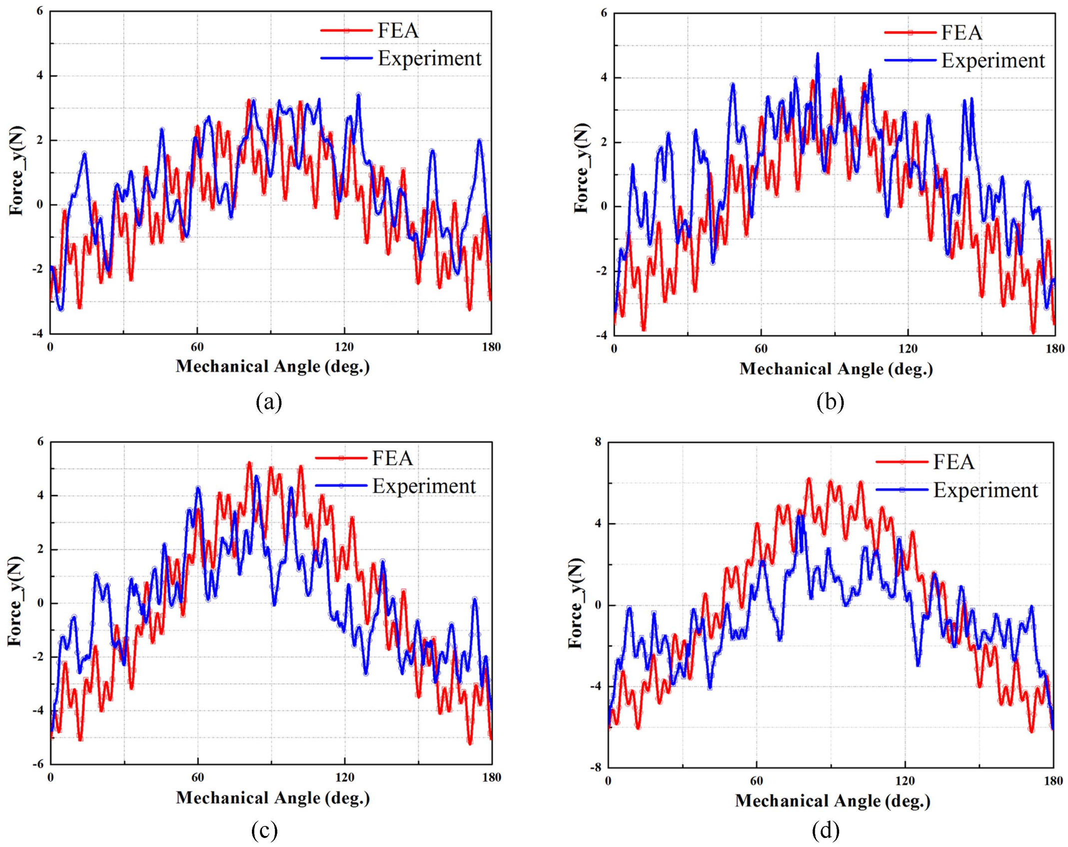

Fig. 7. (Color online) Comparison between measured and simulation results due to rotor eccentricity: (a) 20 μm; (b) 40 μm; (c) 60 μm; (d) 80 μm.

Table 4. Comparison between simulation and measurement results.

Item	Rotor eccentricity			
	20 μm	40 μm	60 μm	80 μm
FEA	6.53 (N)	7.85 (N)	10.49 (N)	12.48 (N)
Experiment	6.87 (N)	8.21 (N)	9.47 (N)	10.47 (N)

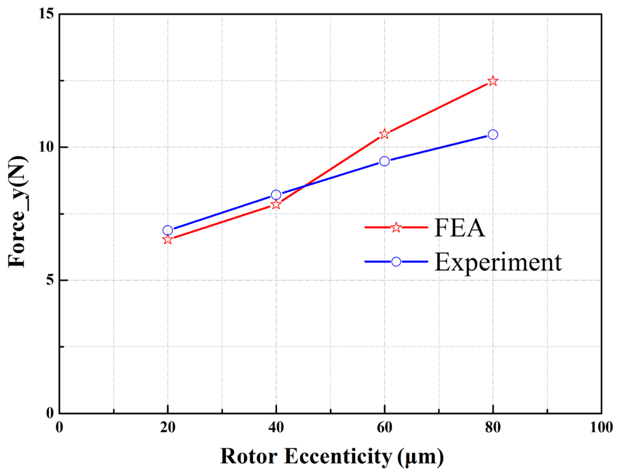

Fig. 8. (Color online) Variation of UMF (peak to peak) with different rotor eccentricity values.

we proposed an experimental setup for the force. We performed a measurement experiment for the y-axis direction force according to a rotor eccentricity of 20 to 80 μm. Subsequently, we compared the measured results to the simulation results obtained by FE analysis S/W. Figure 7 shows the simulation and measured results of UMF according to a rotor eccentricity of 20 to 80 μm. We confirmed that the measured results were similar to the simulation results within the low error. Table 4 presents the result of comparing the simulation values to the measured values by considering an eccentricity of 20 to 80 μm. As the magnitude of rotor eccentricity increased, the difference between the measured results and the simulation results also increased. Figure 8 shows the variation of UMF according to the different values of rotor eccentricity. We confirmed that both the measured and simulation results indicate a linear increase with rotor eccentricity. For the rotor eccentricity of 80 μm, the UMF simulation and measured results show a somewhat higher difference of 16 %. When the rotor eccentricity increased in the PM machine, it was considered that the considerable difference between the simulation and measured results was caused by the measurement error of the load cell itself.

6. Conclusion

In this study, we investigated the prediction and measurement of rotor eccentricity in the PM machine. First, we presented, experimentally and numerically, the UMF characteristics due to rotor eccentricity in the PM machine. The analysis of the characteristics due to rotor eccentricity was performed using FE analysis, while the simulation results indicated the influence of rotor eccentricity on the characteristics of the PM machine. Then, we proposed an experimental set-up in order to measure the UMF according to the variation of rotor eccentricity. The measurement results of UMF due to rotor eccentricity were compared to the simulation results obtained by FE analysis. Consequently, the UMF measurement results obtained by the proposed experimental setup confirmed the validity of the setup for measuring the UMF characteristics due to rotor eccentricity.

References

[1] J. T. Li, Z. J. Liu, and H. A. Nay, Proc. IEEE Trans. Magn. **63**, 2525 (2007).

[2] D. G. Dorrell, M. F. Hsieh, and Y. G. Guo, IEEE Trans. Magn. **45**, 4587 (2009).

[3] B. M. Ebrahimi, J. Faiz, and M. J. Roshtkhari, IEEE Trans. Ind. Electron. **56**, 4727 (2009).

[4] Z. Q. Zhu and David Howe, IEEE Trans. Energy Conversion **15**, 407 (2000).

[5] Yang Zhou, Xiaohua Bao, Chong Di, and Lang Wang, IEEE Trans. Magn. **52**, Art.8202604 (2016).

[6] N. Bianchi and S. Bolognani, IEEE Trans. Ind. Appl. **38**, 1259 (2002).

[7] K. J. Meessen, J. J. H. Paulides, and E. A. Lomonova, IEEE Trans. Magn. **49**, 536 (2013).

[8] J. Y. Kim, S. J. Sung, and G. H. Jang, IEEE Trans. Magn. **48**, 3001 (2012).

[9] C. I. Lee and G. H. Jang, IEEE Trans. Magn. **44**, 4377 (2008).